

DAMPING OF FLUCTUATIONS IN A LASER BEAM PROPAGATING IN SNOWFALLS

A.G. Borovoi, N.A. Vostretsov, A.F. Zhukov, B.A. Kargin, and S.M. Prigarin

*Institute of Atmospheric Optics,
Siberian Branch of the Russian Academy of Sciences, Tomsk
Computer Center,
Siberian Branch of the Russian Academy of Sciences, Novosibirsk
Received December 16, 1996*

The experimental data are presented demonstrating that when laser radiation propagates through a snowfall, its intensity fluctuations are damped starting from a certain distance and (or) with the increase of a snowfall intensity. The model of radiation fluctuations in precipitation proposed earlier by us was applied to interpret the experimental results. According to this model, the multiply scattered field can be divided into the field multiply diffracted on particles' contours and the refracted field. Fluctuation damping factor in this case is defined as the intensity ratio of these fields. The damping factor was computed using the Monte Carlo method.

1. EXPERIMENTAL DATA

As known,^{1,2} intensity fluctuations of radiation propagating in the turbulent atmosphere in their character can be subdivided into the following two regions: the region of weak fluctuations and the region of strong ones. Typical for the first region are short paths or small value of the structural constant C_n^2 of the turbulent atmosphere in this case the scintillation index

$$\beta^2 = (\langle I^2 \rangle - \langle I \rangle^2) / \langle I \rangle^2 \quad (1)$$

increases steadily with increasing either the path length L or the parameter C_n^2 . Here I is the radiation

intensity and the angular brackets $\langle \dots \rangle$ denote statistical averaging. Otherwise, in the region of strong fluctuations, when $L \rightarrow \infty$ and/or $C_n^2 \rightarrow \infty$, the scintillation index tends to $\beta \rightarrow 1$, i.e. saturation of the intensity fluctuations takes place.

If there is precipitation in the atmosphere, then intensity fluctuations show different regularities. Thus, Fig. 1 demonstrates the dependence of the scintillation index in snowfall on the snowfall optical depth τ , obtained by us. As a radiation source, we used a He-Ne laser with the output beam diameter of 3 mm and angular divergence $2\gamma = 5 \cdot 10^{-4}$ rad. The photoreceiver with the receiving area of 0.1 or 0.3 mm was placed on the beam axis. The path length varied from 37 to 1936 m.

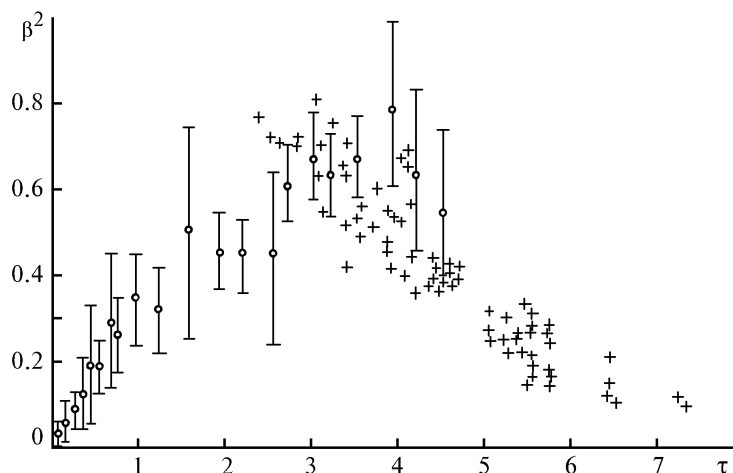


FIG. 1. Scintillation index versus the snowfall optical depth. Snowfall particles mean diameter 1–3 mm; receiver diameter: 0.1 or 0.3 mm (°), 0.3 or 0.5 mm (+).

As seen, in this case intensity fluctuations can be subdivided into three regions. The first region is the region of weak fluctuations, where the scintillation index increases steadily with increasing either the path length L or the precipitation intensity. Then, with increasing path length, the region of fluctuation saturation manifests itself. As was shown in Refs. 3 and 4, here, in contrast to the case of purely turbulent atmosphere, the scintillation index saturates now not at the level of unity, but at some random value, which is mainly determined by the average size of precipitation particles. And then, with further increase in either path length or the precipitation intensity, the scintillation index starts to decrease.⁵ We call this region, having no analogs with the case when radiation propagates in the turbulent atmosphere, the region of fluctuation damping.

2. MODEL OF FLUCTUATIONS WHEN RADIATION PROPAGATES IN PRECIPITATION

The theoretical calculations of the scintillation index at wave propagation in randomly inhomogeneous media is rather a cumbersome mathematical problem, because it requires seeking the fourth momentum of a field. By now such calculations are done only for the case of purely turbulent atmosphere. That is why in Refs. 3 and 4, when interpreting intensity fluctuations in the region of fluctuation saturation, we used a simplified physical model, that yielded sufficiently good general agreement with the experimental data. In this paper we use the same model for interpreting fluctuations in the region of their damping.

The aforementioned model of fluctuations is based on splitting the field, scattered by a precipitation particle, into two qualitatively different components:

$$\mathbf{E} = \mathbf{E}_\partial + \mathbf{E}_n. \quad (2)$$

Here, the first component \mathbf{E}_∂ by definition is a field diffracted on the particle contour. In the wave zone, i.e., at distances $r \gg s$ (where

$$s = kd^2, \quad (3)$$

$k = 2\pi/\lambda$, λ is the wavelength and d is the particle diameter), the field \mathbf{E}_∂ is a diverging spherical wave, concentrated in small scattering angle $\theta = \lambda/d$. At a distance $r \approx s$ from a particle the field \mathbf{E}_∂ is the result of Fresnel diffraction on a particle contour. And, finally, in the near zone $r \ll s$ this field is localized behind the particle, resulting in the geometrical shadow. That is why the field \mathbf{E}_∂ can be called, depending on the situation considered, as diffracted, small-angle, or shadow-forming field.

Let us now consider another field component, \mathbf{E}_n . Since in the particle near zone the scattered field is described by the geometric optics, the field in the near zone is the result of ray reflection and refraction inside the particle. In the wave zone the field \mathbf{E}_n

also transforms into a diverging spherical wave, but this field will be sufficiently large at practically any scattering angle. Therefore the field \mathbf{E}_n can be called either refracted or quasi-isotropic field.

The superposition (2) is valid also for the field scattered by an ensemble of precipitation particles. Here the field \mathbf{E}_n is the result of multiple diffraction at a particles' contours if particles are in the wave zone of each other. If particles are in the far zone of each other, then, in accordance with the value of \mathbf{E}_∂ field behind a particle, the multiply scattered field \mathbf{E}_∂ is the result of multiple mutual shading of particles. Correspondingly, the field \mathbf{E}_n in the scattering medium is the result of multiple ray reflection and refraction in particles, if particles are in the near zone of each other.

It is clear that at a large distance from particles the field \mathbf{E}_n forms the quasi-isotropically diverging spherical wave, while the field \mathbf{E}_∂ at such distances manifests itself as a small-angle peak.

Let us consider now the intensity fluctuations of the multiply scattered field described by the superposition (2). It is known^{1,2} that superposition of a large number of isotropically scattered waves is the Gaussian field with zero mean and scintillation index equal to unity. The correlation length of intensity of such a field inside the scattering medium is small, it is of the order of wavelength. The same regularities also show themselves in the quasi-isotropic multiply scattered field \mathbf{E}_n , which can be approximately presented as a superposition of waves, isotropically diverging from every particle. The correlation length of intensity of \mathbf{E}_n field will be thus of the order of wavelength, and such fluctuations cannot be detected in common measuring schemes.

As a result, the proposed model of fluctuations assumes that in superposition (2) the field \mathbf{E}_∂ is fluctuating in the scattering medium, while the field \mathbf{E}_n is nonfluctuating.

Let us consider the fluctuations of \mathbf{E}_∂ field. If all particles of a scattered medium are at a distance $r \gg s$ from the radiation receiver, then the field \mathbf{E}_∂ at the receiver also is the superposition of diverging spherical waves. But, in contrast to the field \mathbf{E}_n , these spherical waves are strongly anisotropic, i.e. concentrated within small scattering angles. Although the field \mathbf{E}_∂ in this case are Gaussian as before and its scintillation index is equal to unity, the intensity correlation length increases here, that makes fluctuations much better observable in the experiment. According to Ref. 6, the intensity correlation length can be estimated here as $\rho \approx d/\tau$ at $\tau > 1$ and $\rho \approx d$ at $\tau < 1$, where τ is the medium optical depth.

Note that just the superposition of strongly anisotropic spherical waves results in superposition of the scintillation index at the level of unity in the purely turbulent atmosphere.

Really, inhomogeneities of the refractive index of a turbulent atmosphere, taking place in the near

zone of radiation receiver, do not affect intensity fluctuations, because they are equivalent to phase screens. Thus the intensity fluctuations are formed by scattered spherical waves coming from far inhomogeneities. Just these waves form the Gaussian field at a radiation receiver.

The opposite situation takes place in the case of precipitation particles. Here particles from the layer at $r < s$ adjacent to the receiver act as amplitude screens, that in fact corresponds to multiple shadowing of radiation receiver and particles by other particles. Thus the effects from particles from the far layer $r \gg s$ and that adjacent to the radiation receiver are different. According to Refs. 3, 4, and 6 the particles from the adjacent layer result in non-Gaussian statistics, where the blinking index grows infinitely with increasing τ and where the intensity correlation length is of the order of d . As a result, the intensity fluctuations observed under radiation propagation in precipitation are determined by the field \mathbf{E}_δ and are mainly caused by particles from the layer adjacent to the radiation receiver.

Let us apply the above ideas to interpretation of experimental results in the region of fluctuation damping. To this end, we now turn to square field parameters, namely, to the radiation intensity $I(\mathbf{r}, \mathbf{n})$, where \mathbf{n} is the direction of photon motion at a given point \mathbf{r} of space. According to Ref. 6, the interference between fields \mathbf{E}_δ and \mathbf{E}_n can be neglected. Then the radiation intensity also can be separated into the fluctuating part I_δ and nonfluctuating one I_n , each of which is formed by the corresponding components of superposition (2)

$$I(\mathbf{r}, \mathbf{n}) = I_\delta(\mathbf{r}, \mathbf{n}) + I_n(\mathbf{r}, \mathbf{n}). \tag{4}$$

In real measurements the observable value is usually some integral of the radiation intensity, not the radiation intensity itself. Let us call this integral as the measured signal

$$S = \int I(\mathbf{r}, \mathbf{n}) A(\mathbf{r}, \mathbf{n}) \, d\mathbf{r} \, d\mathbf{n}, \tag{5}$$

where A is some instrumental function. Then any measured signal will be separated into the fluctuating and nonfluctuating parts, determined respectively by the radiation intensities I_δ and I_n . Let the scintillation index of the signal resulting from the intensity I_δ be equal

$$\beta_\delta^2 = (\langle S_\delta^2 \rangle - \langle S_\delta \rangle^2) / \langle S_\delta \rangle^2. \tag{6}$$

Then the scintillation index of the whole signal will be lower at the cost of nonfluctuating part resulting from the radiation intensity I_n

$$\beta^2 = \beta_\delta^2 [1 / (1 + S_n / \langle S_\delta \rangle)^2] \equiv \beta_\delta^2 K. \tag{7}$$

Just the equation (7) is final expression for the scintillation index of signals measured in precipitation. Within the considered model of intensity fluctuations the parameter β_δ^2 will be either

steadily increasing or saturating function, while the factor K is the factor of fluctuation damping.

3. NUMERICAL CALCULATION OF THE FACTOR OF FLUCTUATION DAMPING

The factor K of fluctuation damping in Eq. (7) is expressed via the mean components of the radiation intensity $\langle I_\delta(\mathbf{r}, \mathbf{n}) \rangle$ and $I_n(\mathbf{r}, \mathbf{n})$. As known, the statistically mean radiation intensity $\langle I(\mathbf{r}, \mathbf{n}) \rangle$ is described by the radiative transfer equation. Note that the radiative transfer equation successfully describes both multiple rescattering of spherical waves, typical of the field \mathbf{E}_n , and multiple particle shading of each other, characteristic of the field \mathbf{E}_δ . Really, for the intensity $\langle I_\delta(\mathbf{r}, \mathbf{n}) \rangle$ the radiative transfer radiation transforms into the small-angle approximation of the transfer equation. But, as known, the small angle approximation of the radiative transfer equation can be applied to particles both in the near and wave zones of each other, therefore there is no need to distinguish between the particles by distance between them and by distance to the radiation receiver when solving the radiative transfer equation.

The components $\langle I_\delta(\mathbf{r}, \mathbf{n}) \rangle$ and $I_n(\mathbf{r}, \mathbf{n})$ can easily be separated in numerical solution of the radiative transfer equation. Let us substitute the scattering phase function into the radiative transfer equation as a superposition

$$p = p_\delta + p_n. \tag{8}$$

Then that terms of iteration series, which are formed only by the scattering phase functions p_δ , form the radiation intensity $\langle I_\delta(\mathbf{r}, \mathbf{n}) \rangle$. The rest terms, into which the function p_n enters at least one time, correspond to the radiation intensity $I_n(\mathbf{r}, \mathbf{n})$.

In this paper we solved the radiative transfer equation using the Monte Carlo method.⁷ As a measured signal we took the irradiation at a beam axis

$$S = \int I(\mathbf{r}, \mathbf{n}) \mathbf{N} \, d\mathbf{n}, \tag{9}$$

where \mathbf{N} is the normal to the area perpendicular to the optical axis. Since the explicit form of the scattering phase function of snow particles is unknown, as a first approximation we took the simplest function

$$p_n(\mu) = 1/8\pi, \\ p_\delta(\mu) = \begin{cases} [4\pi(1 - \mu_0)]^{-1} & \text{for } \mu = \cos\theta > \mu_0 = \cos\theta_0, \\ 0 & \text{for } \mu < \mu_0, \end{cases} \tag{10}$$

i.e., the quasi-isotropic part of the scattering phase function was taken isotropic, and the small-angle part was taken constant, different from zero in the diffraction cone with the angle $\theta_\delta = \lambda/d$ about the optical axis, where d is the mean diameter of snow particles.

The calculations were made by the method of local estimates. In this case the photon trajectories were divided in numerical simulations into two groups: trajectories with multiple small-angle scattering, giving the value $\langle I_s(\mathbf{r}, \mathbf{n}) \rangle$ and trajectories including at least one scattering event with the scattering phase function p_n , giving the value $I_n(\mathbf{r}, \mathbf{n})$.

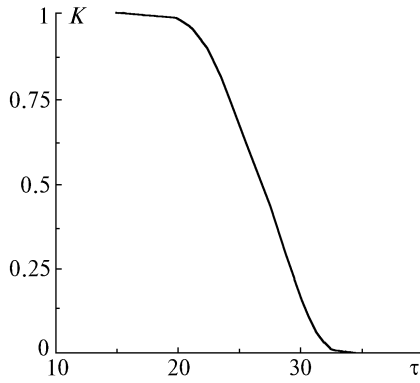


FIG. 2. Fluctuation damping factor as a function of the optical depth.

Figure 2 shows the calculational results for the following parameters, most close to the parameters taking place in our experiments, namely, the He-Ne-laser beam with the divergence $2\gamma = 7 \cdot 10^{-4}$ rad passes the 1-km long path. The point radiation receiver was placed at the beam axis. The radiation source was 1 m from a snowfall, while the receiver was 2.5 m from snowfall, that corresponds to the parameters of the experimental set up. In addition, this condition decreased the variance of calculated values. The mean particle diameter was taken equal to 1 mm, i.e., $\theta_0 = 6 \cdot 10^{-4}$ rad.

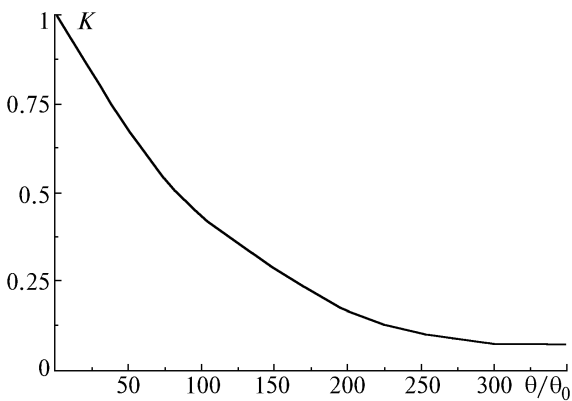


FIG. 3. Fluctuation damping factor as a function of the beam angular divergence, $\theta_0 = 6 \cdot 10^{-4}$ rad.

As seen, under the given experimental conditions the fluctuation damping factor calculated by Eqs. (7)–(10) becomes significant starting from the

optical depth $\tau = 25$, and fluctuation are fully damped at $\tau = 32$.

Intensity fluctuations can also be damped by increasing the beam angular divergence. To numerically estimate this effect, we have calculated the factor K at the same parameters of the experimental setup and the snowfall optical depth $\tau = 10$. As is seen from Fig. 3, the factor K becomes significant, if the angular divergence of a laser beam used is increased by a factor of 50, while fluctuation disappear at the angular divergence increased by a factor of 350.

4. DISCUSSION

According to the experimental data shown in Fig. 1, the region of fluctuation damping begins at $\tau = 5$, while our calculations give a five times greater value. Such a big discrepancy between the experimental and calculated data requires both further refinement of the model of fluctuations and new experimental research.

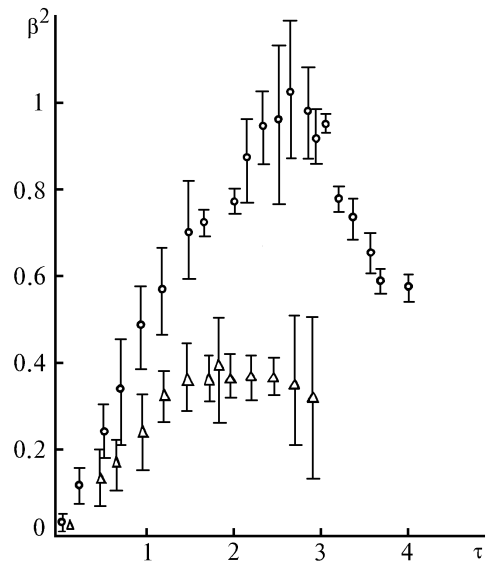


FIG. 4. Scintillation index at large receiver diameter: 0.8 (o) and 3.1 mm (Δ)

Let us note possible causes of this discrepancy between the model and the experiment. First, it is likely that the estimate of intensity correlation length $\rho \approx d$, created by the layer adjacent to the receiver, is overestimated, since it does not take into account the degrees of spatial coherence of the field incident onto this layer. In this case the fluctuation damping observed at Fig. 1 is caused not by increasing contribution from the component $I_n(\mathbf{r}, \mathbf{n})$, but simply by averaging effect of the receiving diaphragm. The experimental data from Fig. 4 obtained under the same conditions as the data from

Fig. 1 but at different diameters of receiving diaphragm favor this assumption. In this case the region of fluctuation damping manifested itself at lower values of the path optical depth.

Second, in numerical calculations of the damping factor K we used the isotropic scattering phase function p_n . If the real scattering phase function is noticeably asymmetric toward the forward hemisphere, then the calculated boundary of the region of fluctuation damping shifts toward smaller optical depths, that can make experimental and model results more close.

ACKNOWLEDGMENT

This work was supported in part by the Russian Foundation for Fundamental Research (project No. 96-02-16388a).

REFERENCES

1. S.I. Rytov, Yu.A. Kravtsov, and V.I. Tatarskii, *Introduction into Statistical Radiophysics* (Nauka, Moscow, 1978), 463 pp.
2. A. Ishimaru, *Wave Propagation and Scattering in Random Media* (Academic Press, New York, 1978).
3. A.G. Borovoi, A.F. Zhukov, and N.A. Vostretsov, *J. Opt. Soc. Am.*, **A12**, 964–969 (1995).
4. A.G. Borovoi, G.Ya. Patruchev, and A.F. Zhukov, *Atmospheric Propagation and Remote Sensing II*, *Proc. SPIE* **1968**, 282–292 (1993).
5. A.F. Zhukov, *Atmos. Oceanic Opt.* **6**, No. 1, 19–21 (1993).
6. A.G. Borovoi, *Izv. Vyssh. Uchebn. Zaved. SSSR, Ser. Radiofiz.* **25**, No. 4, 391–400 (1982).
7. G.I. Marchuk, ed., *Monte Carlo Method in Atmospheric Optics* (Nauka, Novosibirsk, 1976), 281 pp.